

Review Article

The Electrical Bidomain Model: A Review

Sunil M Kandel, PhD

Department of Physics, Oakland University, Rochester, Michigan

***Corresponding author**

Sunil M Kandel.

Email: smkandel@umich.edu

Abstract: Bidomain model is a mathematical representation of the anisotropic electrical properties of cardiac tissue. It is used to simulate cardiac electrical tissue computationally and to study the stimulation of cardiac tissue and defibrillation of the heart. The model is developed using realistic physiological parameter values based on experimental measurement. The first part of this review describes the brief history and development of the bidomain model followed by the formulation of the bidomain equations. The third part of this review presents under what conditions the bidomain model reduces to the monodomain model and discusses its advantages and limitations over the bidomain model. The influence of boundary conditions at the interface between cardiac tissue and an adjacent conductor is described in the fourth part. In the fifth part the properties of cardiac tissue and its relation to conductivity tensors are presented. The bidomain model has successfully predicted many effects of electrical stimulation of the heart. Its limitations and the validity of its predictions to measurements obtained mostly using optical mapping are described in subsequent sections.

Keywords: Bidomain model, cardiac tissue, computer simulation, electrical stimulation, defibrillation.

INTRODUCTION

The bidomain model of cardiac tissue was first suggested by Otto Schmitt [1] and was further developed by several researchers in late 1970s [2-4]. No rigorous derivation of the bidomain model was performed as of 1980. Early papers did not present any connection of the macroscopic equations to the microstructure and to the anisotropic properties of the tissue. Calculations by Plonsey and Barr [5,6] in mid 1980s and several researchers in late 1980s [7-9] established the model as an important tool for analyzing cardiac tissue. In 1989, Sepulveda et al.'s calculation of the transmembrane potential during electrical stimulation [10] introduced the use of the model for understanding pacing and defibrillation. The review by Henriquez [11] remains a useful overview of the bidomain model with more recent reviews found in Wikswo and Roth [12], Henriquez et al. [13], and Trayanova et al. [14]. These are all chapters in the book *Cardiac Bioelectric Therapy: Mechanisms and Practical Implications*.

Neu and Krassowska [15] first derived a homogenized syncytium model (reaction-diffusion equations) from the microstructure and basic physical principles and found that the bidomain model is a special case of the homogenized syncytium model. They derived this model by considering an idealized, periodic representation of the tissue microstructure consisting of cells connected by low resistance junctions and surrounded by extracellular fluid. They

defined a few fundamental material constants in each idealized structure such as conductivities of the cytoplasm inside the cells (σ_i) and the interstitial fluid outside the cells (σ_e), surface specific resistivity of the membrane that separates the inside and outside of the cells (R_m), capacitance of the membrane (C_m) and a typical measure of the cell dimension (d_{cell}). By using these five fundamental material constants, they formulated several additional time and length constants. They treated the potentials inside and outside of the membrane separately and considered them as the solutions to Laplace equations in their respective domains. The electrical properties of the membrane were represented by the boundary conditions that were applied to intra- and extracellular potentials. With all these considerations, they derived a homogenized syncytium model that was represented in the form of reaction-diffusion equations.

Cardiac muscle cells are called myocytes. Each cell is roughly circular cylindrical in shape, typically 30 – 100 μm long and 8 – 20 μm wide. The cells are stacked tightly together in nonuniform layers and are connected to adjacent cells through intercellular channels located at the gap junction. Gap junctions provide intercellular communication by allowing the movement of small molecules, ions and electrical impulses from the intracellular space of one cell to its adjoining cells. A gap junction is composed of two hemichannels called connexons, one in each cell, that come together and form a pore, which establishes

electrical connectivity between the cells [16]. The number of gap junctions between cells determines the electrical properties or conductance of the cardiac tissue.

The heart has on the order of 10^{10} cardiac cells. In modeling the electrical behavior of such cells, the discrete cellular structure is replaced by an averaged continuum that represents the heart. Continuum models of cardiac tissue have several advantages over discrete models, including ease in describing current flowing in both spaces in three dimensions and in applying numerical schemes such as finite difference and finite elements to solve the complex cardiac geometries.

The bidomain model approximates the average electrical behavior of many cells rather than describing each cell individually. Hence the bidomain model is a continuum model. In the bidomain model, the microstructure of cardiac tissue is replaced by intracellular and extracellular continua, each filling the space occupied by the actual tissue. The parameters of the continua are derived by a suitable average of the

cellular structure. Both spaces are described by the same coordinate system. The membrane separates both domains at each point. Hence the bidomain model is the most realistic mathematical expression for macroscopic simulation of cardiac muscle.

The bidomain model is also a multi-dimensional cable model. Figure 1 shows the one dimensional bidomain model. It is represented by rows of resistors coupled through the parallel resistor and capacitor that corresponds to the membrane [17]. If the extracellular resistors were replaced by a zero resistance wire, the one dimensional bidomain model reduces to a monodomain model.

A two dimensional bidomain consists of two domains, the intracellular and extracellular, as shown in Figure 2. Each domain is represented by a network of resistors. The lower grid represents the intracellular domain and the upper grid represents the extracellular domain. Both domains are coupled by resistor and capacitor combinations representing the membrane.

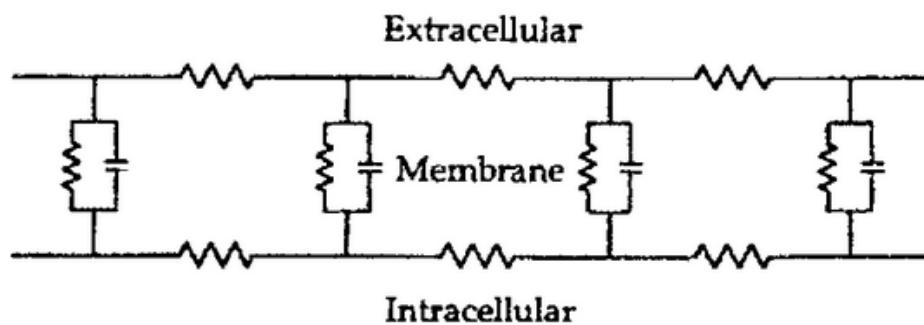


Fig-1: A circuit representation of the one-dimensional cable model. The membrane is represented by the parallel resistors and the capacitors placed between intracellular and extracellular resistors. Reproduced with permission from Roth [17].

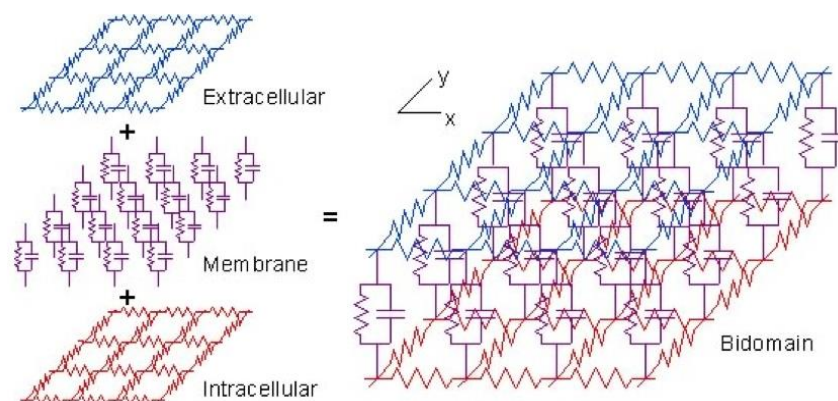


Fig-2: A circuit representation of the two-dimensional cable model. The lower and upper two-dimensional resistor networks parallel to the x-y plane represent the electrical properties of the intracellular and extracellular domains. The vertical resistors and capacitors represent the electrical properties of the membrane.

The Intracellular and extracellular spaces have different electrical conductivities. Both of these spaces are in general anisotropic and hence they have a different electrical conductivity in the direction parallel to the myocardial fibers (the longitudinal direction) than

in the direction perpendicular to them (the transverse direction). Moreover, the degree of anisotropy is different in the two spaces. In the intracellular space, the conductivity parallel to the fibers is about ten times greater than the conductivity perpendicular to the fibers

(10:1), whereas in the extracellular space the ratio is only about 2.5:1. This indicates that the intracellular space is more anisotropic than the extracellular space [18]. This condition of unequal anisotropy ratios in the bidomain model leads to many of the interesting and unexpected stimulus induced responses.

FORMULATION OF BIDOMAIN EQUATIONS

The bidomain equations can be formulated from Ohm’s law and the continuity equation in each domain. The continuity equations are

$$\nabla \cdot J_i = -I_m \tag{1}$$

$$\nabla \cdot J_e = I_m \tag{2}$$

where J_i and J_e are the current densities (A/m²) in the intracellular and extracellular domains and I_m is the membrane current per unit volume (A/m³). The negative sign in equation (1) is a sign convention indicating that the current leaving the intracellular domain is positive. Adding equations (1) and (2) gives $\nabla \cdot (J_i + J_e) = 0$. (3)

Equation (3) implies the conservation of total current.

The membrane current is composed of a capacitive current (I_c) due to the dielectric nature of the cell membrane and an ionic current (I_{ion}) due to currents flowing through different ion channels, pumps and exchangers. Hence

$$I_m = I_c + I_{ion} .$$

But $I_c = \beta C_m \frac{\partial V_m}{\partial t}$ and $I_m = \beta C_m \frac{\partial V_m}{\partial t} + I_{ion}$.

In the passive model the membrane current is given by

$$I_m = \beta \left(C_m \frac{\partial V_m}{\partial t} + G_m V_m \right) , \tag{4}$$

where V_m is the transmembrane potential (mV), β is the ratio of membrane surface area to tissue volume (surface-to-volume ratio) (1/m), C_m is the membrane capacitance per unit area (F/m²), and G_m is the membrane conductance per unit area (S/m²). These equations govern the passive behavior of cardiac tissue when ion channels are not opening and closing. In the passive model, an electrical stimulus does not cause an action potential to propagate.

For active tissue capable of supporting propagation of action potential wave fronts, the term containing $G_m V_m$ is replaced by an Ionic current (I_{ion}), which consists of more complex, nonlinear terms in the form of several ordinary differential equations that specify how the ion channels in the cell membrane respond to changes in the transmembrane potential. This set of coupled ODEs is solved numerically using the Forward Euler method. I_{ion} consists of several sodium, potassium, calcium, pump and exchange currents. The Beeler-Reuter model [19], the Luo-Rudy model [20, 21], and the TNNP model [22] are some of the active membrane models used to study the propagation of action potentials in cardiac tissue.

The transmembrane potential can be written in terms of the extracellular (V_e) and intracellular (V_i) potentials as

$$V_m = V_i - V_e . \tag{5}$$

Similarly, the current densities in the intracellular and extracellular domains can be written in terms of intracellular and extracellular potentials as

$$J_i = -\tilde{g}_i \nabla V_i \tag{6}$$

$$J_e = -\tilde{g}_e \nabla V_e , \tag{7}$$

where \tilde{g}_i and \tilde{g}_e are the intracellular and extracellular conductivity tensors (S/m).

Using equations (6) and (7) in equation (3), and eliminating V_i in favor of V_e and V_m , yields

$$\nabla \cdot [(\tilde{g}_i + \tilde{g}_e) \nabla V_e] = -\nabla \cdot (\tilde{g}_i \nabla V_m) . \tag{8}$$

Equation (8) is one of the bidomain equations.

Inserting equation (4) to equation (2) and replacing $G_m V_m$ by I_{ion} gives

$$\nabla \cdot (\tilde{g}_e \nabla V_e) = -\beta \left(C_m \frac{\partial V_m}{\partial t} + I_{ion} \right) . \tag{9}$$

Rewriting equation (9) gives another bidomain equation

$$C_m \frac{\partial V_m}{\partial t} = -I_{ion} - \frac{1}{\beta} \nabla \cdot \tilde{g}_e \nabla V_e . \tag{10}$$

I_{ion} is the membrane ion current (where the Luo-Rudy model enters the equations). Equations (8) and (10) are coupled partial differential equations and are the final bidomain equations.

Equation (10) depends explicitly on time, is nonlinear because of I_{ion} , and has properties similar to a parabolic partial differential equation (a reaction-diffusion system). I_{ion} describes the total ionic current in the form of several ordinary differential equations and is solved numerically by Euler's method. Equation (8) has no explicit time dependence, and is an elliptic partial differential equation (a boundary value problem) that is usually challenging to solve numerically. These coupled equations are often approximated with finite differences or finite elements. At each time step, equation (10) is used to update V_m and then equation (8) is solved for V_e using the updated V_m in the source term on the right-hand-side.

MONODOMAIN MODEL

The monodomain model describes the current flowing only in the intracellular region of the heart. The bidomain model can be reduced to the monodomain model if we neglect the effect of the extracellular potential or if we consider the case where the anisotropy ratios of both spaces are equal [23].

Assuming equal anisotropy ratios, i.e. $\tilde{g}_e = \lambda \tilde{g}_i$, equation (8) becomes

$$\nabla \cdot [\tilde{g}_i \nabla V_e] = - \frac{1}{(1+\lambda)} \nabla \cdot (\tilde{g}_i \nabla V_m).$$

Inserting this equation into equation (9) gives

$$\frac{\lambda}{(1+\lambda)} \nabla \cdot (\tilde{g}_i \nabla V_m) = \beta \left(C_m \frac{\partial V_m}{\partial t} + J_{ion} \right). \quad (11)$$

Equation (11) is the monodomain equation. It consists of a single parabolic partial differential equation in terms of V_m only. It is a special case of the bidomain model. It needs less processing time, and is less challenging to solve numerically. If we are interested only in wave propagation, the monodomain model is sufficient. However if we consider the effect of the bath, stimuli, and conductivity tensors to make tissue anisotropic, we should use the bidomain model. The bidomain equations are particularly useful for simulations where the extracellular space is important for injecting current, such as investigations of defibrillation shocks [24, 25].

The unequal anisotropy ratios of cardiac tissue results in the characteristic spatial distribution of transmembrane potential during unipolar stimulation of the cardiac tissue [10]. Unipolar stimulation induces adjacent regions of depolarized and hyperpolarized tissue. Cathodal stimulation depolarizes the tissue under the electrode and hyperpolarizes it along the direction of the fibers. Anodal stimulation results in just the opposite arrangement. The regions of depolarization and hyperpolarization are called the virtual cathodes and virtual anodes [26-28].

BOUNDARY CONDITIONS

The electrical properties of cardiac tissue are significantly influenced by the boundary conditions at the interface between cardiac tissue and an adjacent conductor [29, 30]. In our simulation, we use a no-flux boundary condition for cardiac tissue that is electrically isolated from the conductive medium. If the cardiac tissue is surrounded by a conductive medium, such as blood or a perfusing bath, then Laplace's equation has to be solved in addition to the bidomain equations.

We apply a unipolar stimulus current through a cylindrical electrode centered at the origin. It has a length of 1 mm along the z direction (the direction of the myocardial fibers) and a diameter of 0.4 mm along the ρ direction (radially outward, perpendicular to the fibers), and has a surface area of 1.51 mm². Three boundary conditions are applied at the tissue-electrode interface: the normal component of the intracellular current density is zero; the extracellular potential is constant; and the total current passing from the electrode into the extracellular space is equal to the stimulus current [29]. At the tissue's outer edge, the normal component of the intracellular current density is zero and the extracellular potential is zero. During unipolar cathodal stimulation, the outer edge of the tissue behaves as the anode and has negligible influence on the electrical behavior near the stimulating electrode.

BIDOMAIN PROPERTIES

Since cardiac cells are not uniform, it is difficult to determine the conductivity tensors (conductivities) associated with the intra- and extracellular spaces. Conductivity tensors vary spatially. Different researchers estimate different values of the conductivity tensors, examine the effects produced by them and try to correlate them with macroscopic experiments. Bidomain conductivities have been measured experimentally but the values are inconsistent [31-33] (Table 1). One could not get accurate values of the conductivity tensors unless microscopic properties of the tissue are completely known, such as the resistance of the gap junctions. The resistance of the cardiac tissue depends on the number of gap junctions between the cells. Since different connexin proteins are found in different regions of the heart, it is difficult to find accurate values of the conductivity tensors. The measured values of the resistance of gap junctions vary widely in the literature, ranging from 0.5 to 40 M Ω . In general, the properties of cardiac tissue depend on the cell shape and size, and the gap junction distribution.

Table-1: The bidomain conductivities for ventricular tissue.

Parameter	Symbol	Clerc [31]	Robert et al. [32]	Robert & Scher [33]	Roth [34]	Roth [35]
Intracellular conductivity parallel to the fibers (S/m)	g_{iz}	0.17	0.28	0.34	0.35	0.2
Intracellular conductivity perpendicular to the fibers (S/m)	$g_{i\rho}$	0.019	0.026	0.06	0.03	0.02
Extracellular conductivity parallel to the fibers (S/m)	g_{ez}	0.62	0.22	0.12	0.30	0.2
Extracellular conductivity perpendicular to the fibers (S/m)	$g_{e\rho}$	0.24	0.13	0.08	0.18	0.08
Ratio	$g_{iz}/g_{i\rho}$	8.9	10.8	5.8	11.7	10
Ratio	$g_{ez}/g_{e\rho}$	2.6	1.7	1.5	1.7	2.5

In my simulations using the bidomain equations, conductivities are assumed constant throughout the tissue, which may not be the case for normal and diseased tissue. In general, the orientations of the cells in the heart are not uniform. As a result, the conductivities are heterogeneous. However, my calculations focus primarily on unipolar stimulation with stimulus strengths only a few times threshold. As long as the fiber geometry and direction are constant within a few millimeters around the unipolar electrode, these calculations should be relatively insensitive to the fiber geometry through the rest of the tissue.

VALIDITY OF THE BIDOMAIN MODEL

Neu and Krassowska [15] pointed out the limitations of the bidomain model and argued that the model might not apply when (1) the region of interest is near the tissue surface, (2) the calculated transmembrane potential is significantly greater than the experimental value, (3) the electric field is strong and nonuniform, (4) the phenomena of interest is near the external source and (5) the phenomena of interest occurs on a time scale

of less than 1 ms. Despite its limitations, several bidomain predictions are verified experimentally, as described in the next section.

OPTICAL MAPPING

Numerous experimental and clinical techniques, such as the electrocardiogram in vivo and optical mapping in vitro animal experiments, are used to study the behavior of cardiac tissue. Optical mapping is an imaging technique used to measure the transmembrane potential with high spatial and temporal resolution by using voltage-sensitive fluorescent dyes perfused throughout the tissue. In this technique, the heart is stained with voltage sensitive dye (for example, di-4-ANEPPS). When transmembrane voltage (V_m) changes, the fluorescence of the voltage-sensitive dye will change accordingly. The change in the emitted light is recorded by a photodiode detector array, which is coupled to computerized data acquisition system to convert fluorescence emitted from the tissue to a map of V_m [36]. Figure 3 shows the schematic representation of optical imaging setup.

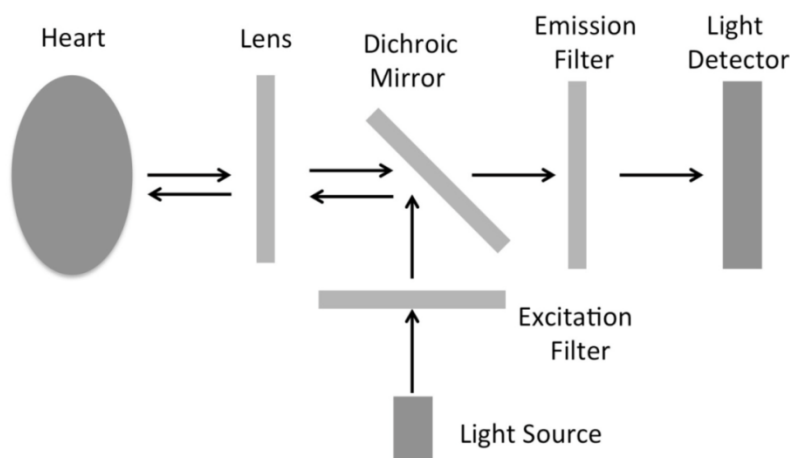


Fig-3: Schematic representation of an optical mapping experimental setup. It has three major components: the perfused heart, the light sources, and the light detector.

BIDOMAIN PREDICTIONS AND EXPERIMENTAL CONFIRMATION

Over the past 20 years, two areas of research – the theoretical study of cardiac tissue using the bidomain model and experimental study of cardiac tissue using optical mapping – have resolved many long-standing questions of cardiology. Several bidomain predictions have been experimentally confirmed. Comparing numerical simulations to experimental data and getting a close match gives us confidence that the model is correct. Wikswo and Roth [12] illustrate the agreement between theoretical predictions of the bidomain model and experiments.

CONCLUSION

The bidomain model is a continuum representation of the two anisotropic spaces of myocardium. It is currently the state-of-the-art model to study the stimulation of cardiac tissue and defibrillation of the

heart [37-41]. Bidomain simulations help us 1) to predict the mechanisms of unipolar stimulation such as make and break excitation and the shape of the strength-interval curve, 2) to understand the mechanism of reentry, 3) to find the response of tissue-shock interaction during defibrillation.

ACKNOWLEDGEMENT

This research was supported by NIH grant R01HL118392.

REFERENCES

1. Schmitt OH; Biological information processing using the concept of interpenetrating domains. In: Leibovic KN, ed. Information Processing in the Nervous System. New York: Springer, 1969: 325-331.
2. Muler AL, Markin VS; Electrical properties of anisotropic nerve-muscle syncytia. I. Distribution

- of the electrotonic potential. *Biophysics*, 1977; 22 (2):07–31.
3. Tung L; A bi-domain model for describing ischemic myocardial D-C potentials Ph.D. thesis. Massachusetts Institute of Technology, Cambridge, Mass, USA, 1978.
 4. Miller WT III, Geselowitz DB; Simulation studies of the electrocardiogram. I. The normal heart. *Circulation Research*, 1978; 43(2):301–315.
 5. Plonsey R, Barr RC; Current flow patterns in two dimensional anisotropic bisyncytia with normal and extreme conductivities. *Biophysical Journal*, 1984; 45(3):557–571.
 6. Barr RC, Plonsey R; Propagation of excitation in idealized anisotropic two dimensional tissue. *Biophysical Journal*, 1984; 45 (6):1191–1202.
 7. Roth BJ, Wikswo JP Jr; A bidomain model for the extracellular potential and magnetic field of cardiac tissue. *IEEE Transactions on Biomedical Engineering*, 1986; 33(4): 467–469.
 8. Wikswo JP Jr., Sepulveda NG; Electric and magnetic fields from two-dimensional anisotropic bisyncytia. *Biophysical Journal*, 1987; 51(4): 557–568.
 9. Plonsey R, Barr RC; Interstitial potentials and their change with depth into cardiac tissue. *Biophysical Journal*, 1987; 51(4): 547–555.
 10. Sepulveda NG, Roth BJ, Wikswo JP Jr; Current injection into a two dimensional anisotropic bidomain. *Biophysical Journal*, 1989; 55 (5): 987–999.
 11. Henriquez CS; Simulating the electrical behavior of cardiac tissue using the bidomain model. *Crit. Rev. Biomed. Eng.*, 1993; 21: 1–77.
 12. Wikswo JP Jr, Roth BJ; Virtual electrode theory of pacing. In: *Cardiac Bioelectric Therapy: Mechanisms and Practical Implications*. I. R. Efimov, M. Kroll, and P. Tchou, Eds., Springer, New York, 2009: 283-330.
 13. Henriquez CS, Ying W; The bidomain model of cardiac tissue: From microscale to macroscale. In: *Cardiac Bioelectric Therapy: Mechanisms and Practical Implications*. I. R. Efimov, M. Kroll, and P. Tchou, Eds., Springer, New York, 2009: 401-421.
 14. Trayanova N, Plank G; Bidomain model of defibrillation. In: *Cardiac Bioelectric Therapy: Mechanisms and Practical Implications*. I. R. Efimov, M. Kroll, and P. Tchou, Eds., Springer, New York, 2009: 85-109.
 15. Neu JC, Krassowska W; Homogenization of syncytial tissues. *Crit. Rev. Biomed. Eng.*, 1993; 21:137–199.
 16. Evans WH, Martin; Gap junctions: structure and function (review). *Mol Membr Biol*, 2002; 19: 121-136.
 17. Roth BJ; How the anisotropy of the intracellular and extracellular conductivities influences stimulation of cardiac muscle. *J. Math. Biol.*, 1992; 30: 633–646.
 18. Roth BJ; Electrical conductivity values used with the bidomain model of cardiac tissue. *IEEE Trans. Biomed. Eng.*, 1997; 44:326-328.
 19. Beeler GW, Reuter H; Reconstruction of the action potential of ventricular myocardial fibers. *J Physiol*, 1977; 268: 177 – 210.
 20. Luo CH, Rudy Y; A model of the ventricular cardiac action potential. Depolarization, repolarization, and their interaction. *Circ Res*, 1991; 68: 1501 – 1526.
 21. Luo CH, Rudy Y; A dynamic model of the cardiac ventricular action potential. I. Simulations of ionic currents and concentration changes. *Circ Res*, 1994; 74: 1071 – 1096.
 22. Ten Tusscher KH, Noble D, Noble PJ, Panfilov AV; A model for human ventricular tissue. *American Journal of Physiology. Heart and Circulatory Physiology*, 2004; 286(4): H1573–H1589.
 23. Keener JP, Sneyd J; *Mathematical Physiology*. 2nd edition, Springer, 2008.
 24. Trayanova N; Defibrillation of the heart: insights into mechanisms from modeling studies. *Experimental Physiology*, 2006; 91(2):323–337
 25. Bernabeu M, Pathmanathan P, Pitt-Francis J, Kay D; Stimulus protocol determines the most computationally-efficient preconditioner for the bidomain equations. *IEEE Transactions on Biomedical Engineering*, 2010.
 26. Knisley SB; Transmembrane voltage changes during unipolar stimulation of rabbit ventricle. *Circulation Research*, 1995; 77(6):1229–1239.
 27. Neunlist M, Tung L; Spatial distribution of cardiac transmembrane potentials around an extracellular electrode: dependence on fiber orientation, *Biophysical Journal*, 1995; 68 (6): 2310–2322.
 28. Wikswo JP Jr., Lin SF, Abbas RA; Virtual electrodes in cardiac tissue: a common mechanism for anodal and cathodal stimulation. *Biophysical Journal*, 1995; 69(6): 2195–2210.
 29. Krassowska W, Neu JC; Effective boundary conditions for syncytial tissues. *IEEE Trans Biomed Eng*, 1994; 41:143–150.
 30. Roth BJ; A comparison of two boundary-conditions used with the bidomain model of cardiac tissue. *Ann Biomed Eng.*, 1991; 19:669–678.
 31. Clerc L; Directional differences of impulse spread in trabecular muscle from mammalian heart. *J. Physiol. (London)*, 1976; 255: 335–346.
 32. Roberts D, Hersch LT, Scher AM; Influence of cardiac fiber orientation on wave front voltage, conduction velocity and tissue resistivity. *Circ. Res.*, 1979; 44:701–712.
 33. Roberts D, Scher AM; Effect of tissue anisotropy on extracellular potential fields in canine myocardium in situ. *Circ. Res.*, 1982; 50:342–351.
 34. Roth BJ; The electrical potential produced by a strand of cardiac muscle: a bidomain analysis. *Ann Biomed Eng*, 1988; 16:609–637.

35. Roth BJ; Nonsustained reentry following successive stimulation of cardiac tissue through a unipolar electrode. *J Cardiovasc Electrophysiol*, 1997; 8:768–778.
36. Rosenbaum DS, Jalife J; Optical mapping of cardiac excitation and arrhythmias, Futura Publishing Company, Inc, 2001.
37. Bishop MJ, Connolly A, Plank G; Structural heterogeneity modulates effective refractory period: A mechanism of focal arrhythmia initiation. *PLOS ONE*, 2014; 9(10): e109754.
38. Colli Franzone P, Pavarino LF, Scacchi S; Effects of premature anodal stimulations on cardiac transmembrane potential and intracellular calcium distributions computed by anisotropic bidomain models. *EUROPACE*, 2014; 16(5): 736-742.
39. Kandel SM, Roth BJ; Intracellular calcium and the mechanism of the dip in the anodal strength-interval curve in cardiac tissue. *Circulation J.*, 2014; 78:1127-1136.
40. Nagaiah C, Kunisch K, Plank G; Optimal control approach to termination of re-entry waves in cardiac electrophysiology. *J Mathematical Biol*, 2013; 67(2): 359-388.
41. Rantner LJ, Tice BM, Trayanova NA; Terminating ventricular tachyarrhythmias using far-field low-voltage stimuli: Mechanisms and delivery protocols. *Heart Rhythm*, 2013; 10(8): 1209-1217.